Available online at www.sciencedirect.com
ScienceDirect
Chemical Physics 329 (2006) 276–282
Chemical Physics
www.elsevier.com/locate/chemphys

A short-range gradient-corrected spin density functional in combination with long-range coupled-cluster methods: Application to alkali-metal rare-gas dimers

Erich Goll [a,*], Hans-Joachim Werner [a], Hermann Stoll [a], Thierry Leininger [b], Paola Gori-Giorgi [c], Andreas Savin [c]

[a] Institut für Theoretische Chemie, Universität Stuttgart, Pfaffenwaldring 55, D-70550 Stuttgart, Germany
[b] Laboratoire de Physique Quantique, UMR 5626 du CNRS, Université Paul Sabatier, 118 Route de Narbonne, F-31062 Toulouse Cedex 04, France
[c] Laboratoire de Chimie Théorique, CNRS UMR7616, Université Pierre et Marie Curie, 4 Place Jussieu, F-75252 Paris, France

Received 2 May 2006; accepted 24 May 2006
Available online 6 June 2006

Dedicated to Professor Lorenz S. Cederbaum on the occasion of his 60th birthday.

Abstract

We extend our recently published short-range gradient-corrected density functional from the closed-shell to the open-shell case, combine it with long-range coupled-cluster methods (CCSD, CCSD(T)), and apply it to the weakly bound alkali-metal rare-gas dimers AmRg (Am = Li–Cs; Rg = Ne–Xe). The results are shown to be superior, with medium-size basis sets, to pure DFT and pure coupled-cluster calculations.

PACS: 31.15.−p; 31.15.Ar; 31.15.Dv; 31.15.Ew

Keywords: Spin density functional; Open-shell coupled cluster; Short-range/long-range separation; Van der Waals systems

1. Introduction

Density functional (DFT) and wave-function based ab initio methods are to some extent complementary. DFT methods, on the one hand, provide a good description of dynamic correlation at a reasonable cost-value ratio, but a systematic improvement is currently not feasible. Ab initio methods, on the other hand, yield a good description of static correlation and can be systematically improved to high accuracy, but large one-particle basis sets are required for the treatment of dynamic correlation.

In order to combine the benefits of both brands of methods, it has been suggested [1–4] to relieve ab initio methods from the description of the interelectronic cusp by splitting off the short-range (*sr*) part of the interelectronic Hamiltonian $\sum_{i<j} 1/r_{ij}$ – which is mainly responsible for their heavy basis-set dependency – and access this part by DFT. Then, only the long-range (*lr*) part of the interelectronic interaction has to be covered by an explicitly wavefunction-based description.

Within this theoretical framework it is necessary to use specially developed *sr* density functionals – so as to avoid double counting of the *lr* part of electron exchange and correlation. We have recently shown [5] that a *sr* gradient-corrected density functional of the Perdew–Burke–Ernzerhof (PBE) type [6] delivers excellent results for the potential curves of rare gas dimers.

In the present paper, we extend this functional, which was designed to handle closed-shell systems, to the

* Corresponding author.
E-mail address: goll@theochem.uni-stuttgart.de (E. Goll).

0301-0104/$ - see front matter © 2006 Elsevier B.V. All rights reserved.
doi:10.1016/j.chemphys.2006.05.020

open-shell case. We furthermore introduce this functional into the open-shell coupled-cluster code (RCCSD(T), UCCSD(T)) [7,8] of the program package MOLPRO [9], treating single, double and triple excitations with respect to a restricted Hartree–Fock (RHF) reference. The method is outlined in Section 2. For demonstrating the accuracy of our new *sr*-PBE/*lr*-CCSD(T) approach, we apply it to the van der Waals bound alkali-metal rare-gas dimers AmRg (Am = Li–Cs; Rg = Ne–Xe), cf. Section 3. Concluding remarks follow in Section 4.

2. Functionals and implementation

The functionals to be described in this section refer to the following separation of the interelectronic interaction operator of the Hamiltonian into long- and short-range parts:

$$\begin{aligned} V_{\mathrm{ee}} &= V_{\mathrm{ee}}^{lr} + V_{\mathrm{ee}}^{sr}, \\ V_{\mathrm{ee}}^{lr} &= \sum_{i<j} \frac{\mathrm{erf}(\mu r_{ij})}{r_{ij}}, \\ V_{\mathrm{ee}}^{sr} &= \sum_{i<j} \frac{1-\mathrm{erf}(\mu r_{ij})}{r_{ij}}, \end{aligned} \tag{1}$$

where erf is the standard error function. The separation of the energy expression into a long-range part to be treated by wavefunction-based ab initio methods and a short-range part to be treated by DFT can readily be done using Levy's constrained-search formalism [10]:

$$\begin{aligned} E_0 &= \min_{\rho}\left(\min_{\Psi\to\rho}\langle\Psi|T+V_{\mathrm{ne}}+V_{\mathrm{ee}}^{lr}|\Psi\rangle + E_0^{sr}[\rho]\right) \\ E_0^{sr}[\rho] &= \min_{\Psi\to\rho}\langle\Psi|T+V_{\mathrm{ee}}|\Psi\rangle - \min_{\Psi\to\rho}\langle\Psi|T+V_{\mathrm{ee}}^{lr}|\Psi\rangle \\ &= U_{\mathrm{H}}^{sr}[\rho] + E_{\mathrm{xc}}^{sr}[\rho]. \end{aligned} \tag{2}$$

Here, E_0 is the ground state energy, U_{H}^{sr} is the *sr* Hartree energy, and E_{xc}^{sr} defines the functional to be approximated. Note that $E_{\mathrm{xc}}^{sr}[\rho]$ is no longer a functional of the electron density ρ alone, it also depends on the coupling parameter μ. For $\mu = 0$, its definition coincides with that of the usual density functional, but for $\mu > 0$ the dependence on ρ will change. For $\mu \to \infty$ the pure coupled-cluster limit is attained.

In this work, we extend our previously proposed PBE-like closed-shell *sr* density functional [5] to the open-shell case. The exchange part of the closed-shell functional reads

$$\begin{aligned} E_{\mathrm{x}}^{sr}[\rho,\nabla\rho] &= \int \mathrm{d}^3 r \rho \varepsilon_{\mathrm{x}}^{\mathrm{LDA}}(\mu,\rho) F_{\mathrm{x}}(\mu,s), \\ F_{\mathrm{x}}(\mu,s) &= 1+\kappa-\frac{\kappa}{1+b(\mu)s^2/\kappa}, \\ b(\mu) &= \frac{b^{\mathrm{PBE}}}{b^{\mathrm{T}}(0)} b^{\mathrm{T}}(\tilde{\mu}) \mathrm{e}^{-\alpha_{\mathrm{x}}\tilde{\mu}^2} \\ s &= \frac{|\nabla\rho|}{2k_F\rho}, \end{aligned} \tag{3}$$

where $\kappa = 0.840$, $b^{\mathrm{PBE}} = 0.21951$ and $k_F = (3\pi^2\rho)^{1/3}$ are parameters already included in the standard PBE functional; $b^{\mathrm{T}}(\tilde{\mu})$ ($\tilde{\mu} = \mu/(2k_F)$) was taken from Ref. [11], and the exponential term with $\alpha_{\mathrm{x}} = 19.0$ was introduced in Ref. [5] for damping off the gradient term in the large μ limit.

Due to the additivity of the exchange energy, the corresponding open-shell functional can be easily obtained via the spin–scaling relationship:

$$E_{\mathrm{x}}^{sr}[\rho_\uparrow,\rho_\downarrow,\nabla\rho_\uparrow,\nabla\rho_\downarrow] = (E_{\mathrm{x}}^{sr}[2\rho_\uparrow,2\nabla\rho_\uparrow] + E_{\mathrm{x}}^{sr}[2\rho_\downarrow,2\nabla\rho_\downarrow])/2, \tag{4}$$

where $\rho_\uparrow/\rho_\downarrow$ are spin-up/down densities.

The correlation part of the closed-shell functional reads

$$\begin{aligned} E_{\mathrm{c}}^{sr}[\rho,\nabla\rho] &= \int \mathrm{d}^3 r \rho [\varepsilon_{\mathrm{c}}^{\mathrm{LDA}}(\mu,\rho) + H(\mu,\rho,t)], \\ H(\mu,\rho,t) &= \gamma \ln\left\{1+\frac{\beta(\mu)t^2}{\gamma}\left[\frac{1+At^2}{1+At^2+A^2t^4}\right]\right\}, \\ \beta(\mu) &= \beta^{\mathrm{PBE}}\left(\frac{\varepsilon_{\mathrm{c}}^{\mathrm{LDA}}(\mu,\rho)}{\varepsilon_{\mathrm{c}}^{\mathrm{LDA}}(0,\rho)}\right)^{\alpha_{\mathrm{c}}}, \\ A &= \frac{\beta(\mu)}{\gamma(\exp(-\varepsilon_{\mathrm{c}}^{\mathrm{LDA}}(\rho,\mu)/\gamma)-1)}, \\ t &= \frac{|\nabla\rho|}{2k_s\rho}, \end{aligned} \tag{5}$$

where $\gamma = 0.031091$, $\beta^{\mathrm{PBE}} = 0.066725$ and $k_s = \sqrt{4k_F/\pi}$ are parameters already included in the standard PBE functional and the μ-dependent factor in $\beta(\mu)$, with $\alpha_{\mathrm{c}} = 2.83$, was used in Ref. [5] to damp off the gradient term for large μ.

The construction of the open-shell correlation functional is more sophisticated than that of the open-shell exchange functional, since correlation affects all electrons and the correlation energy is non-additive for the two spin-systems. The dependence on the spin polarisation $\zeta = (\rho_\uparrow - \rho_\downarrow)/\rho$ has to be included both into the local-spin-density (LDA) part of the functional and into the gradient correction, i.e. $\varepsilon_{\mathrm{c}}^{\mathrm{LDA}}(\mu,\rho) \to \varepsilon_{\mathrm{c}}^{\mathrm{LDA}}(\mu,\rho,\zeta), H(\mu,\rho,t) \to H(\mu,\rho,\zeta,t)$. The LDA functional $\varepsilon_{\mathrm{c}}^{\mathrm{LDA}}(\mu,\rho,\zeta)$ is taken from Ref. [12], the gradient correction $H(\mu,\rho,\zeta,t)$ is built according to Ref. [6] by introducing the spin–scaling factor $\phi(\zeta) = [(1+\zeta)^{2/3} + (1-\zeta)^{2/3}]/2$. Finally, we get

$$\begin{aligned} E_{\mathrm{c}}^{sr}[\rho_\uparrow,\rho_\downarrow,\nabla\rho] &= \int \mathrm{d}^3 r \rho [\varepsilon_{\mathrm{c}}^{\mathrm{LDA}}(\mu,\rho,\zeta) + H(\mu,\rho,\zeta,t)], \\ H(\mu,\rho,\zeta,t) &= \gamma\phi^3 \ln\left\{1+\frac{\beta(\mu)t^2}{\gamma}\left[\frac{1+At^2}{1+At^2+A^2t^4}\right]\right\}, \\ \beta(\mu) &= \beta^{\mathrm{PBE}}\left(\frac{\varepsilon_{\mathrm{c}}^{\mathrm{LDA}}(\mu,\rho,\zeta)}{\varepsilon_{\mathrm{c}}^{\mathrm{LDA}}(0,\rho,\zeta)}\right)^{\alpha_{\mathrm{c}}}, \\ A &= \frac{\beta(\mu)}{\gamma(\exp(-\varepsilon_{\mathrm{c}}^{\mathrm{LDA}}(\mu,\rho,\zeta)/(\gamma\phi^3))-1)}, \\ t &= \frac{|\nabla\rho|}{2\phi k_s\rho}. \end{aligned} \tag{6}$$

The value of α_{c} has to be readjusted to $\alpha_{\mathrm{c}} = 2.78$, because $\varepsilon_{\mathrm{c}}^{\mathrm{LDA}}(\mu,\rho,\zeta)$ is based on improved quantum Monte-Carlo (QMC) calculations and a different fitting procedure (PW92C instead of VWN80).

Finally, we applied our μ-dependent new functionals to the ^{4}S ground state of the N atom so as to check their performance. To this end we plotted the ratio of the exchange energy in the combined *sr*-DFT/*lr*-HF approach to the HF reference value, $(E_x^{DFT}(sr) + E_x^{HF}(lr))/E_x^{HF}$, cf. Fig. 1, and the ratio of the correlation energy in the combined *sr*-DFT/*lr*-CCSD(T) approach to the CCSD(T) energy calculated with large basis set, $(E_c^{DFT}(sr) + E_c^{CCSD(T)}(lr))/E_c^{CCSD(T)}$, cf. Fig. 2. Ideally, the ratio should in both cases be equal to 1, independent of μ. In practice, we encounter the well-documented deficiencies of the standard LDA and PBE functionals at the pure DFT limit ($\mu \to 0$). In particular, standard LDA underestimates (the magnitude of) the exchange energy by ~10% and overestimates correlation by a factor of more than 2. These errors are gradually reduced by mixing in exact exchange/correlation with increasing μ, for $0.1 < \mu < 10$ a.u.. The starting point is much better with standard PBE at $\mu = 0$, and our PBE-like short-range functionals allow to essentially retain this accuracy over the whole range of μ values, with deviations of $< 1\%$ for exchange and $< 6\%$ for correlation.

The above short-range spin density functionals have been implemented into the program package MOLPRO [9]. In the first step, the orbitals are optimised by minimising for the high-spin single-determinant spin-restricted wavefunction Ψ the energy expression:

$$E_0 = \min_{\Psi}\{\langle\Psi|T + V_{ne} + V_{ee}^{lr}|\Psi\rangle + U_H^{sr}[\rho[\Psi]] + E_{xc}^{sr}[\rho[\Psi],\zeta[\Psi]]\}, \quad (7)$$

where $\rho[\Psi]$ and $\zeta[\Psi]$ are the electron density and spin polarisation corresponding to Ψ. This amounts to a hybrid-type restricted Kohn–Sham (RKS) calculation with the *sr* density functional $E_{xc}^{sr}[\rho]$ and *lr* exact exchange. In practice, a RHF calculation is performed, with the standard electron repulsion integrals (ERI) replaced by their *lr* counterparts, and with the *sr* Coulomb operator and the *sr* exchange–correlation potential derived from E_{xc}^{sr} added. In the second step, the still missing *lr* correlation effects are taken into account by performing a coupled-cluster calculation with single, double and perturbative triple excitations of the restricted or unrestricted type (RCCSD(T), UCCSD(T)) [7,8], for the first term on the right-hand side of Eq. (7). Thereby, only *lr* ERIs are used, and the influence of *sr* Coulomb and exchange/correlation is included by means of the relevant *sr* functionals/potentials determined in the first step.

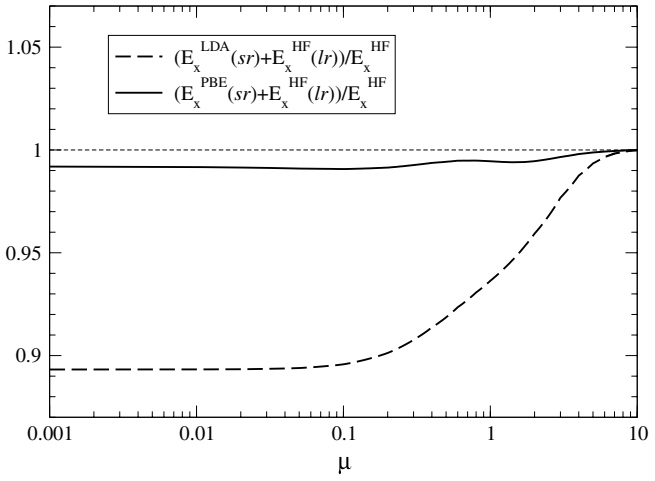

Fig. 1. Approximations for the exchange energy of N (aug-cc-pVQZ basis set), as a function of the coupling parameter μ (a.u.): $(E_x^{DFT}(sr) + E_x^{HF}(lr))/E_x^{HF}$ is the ratio of the mixed *sr*-DFT/*lr*-HF exchange approximation, with the LDA and our modified PBE-like functional, to the full HF exchange energy.

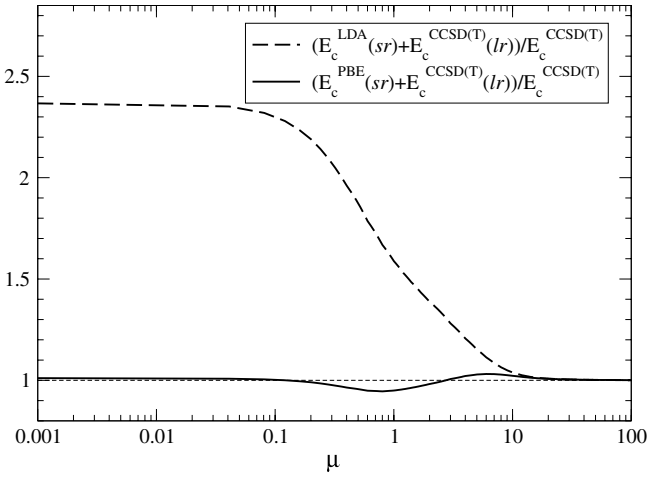

Fig. 2. Approximations for the correlation energy of N (uncontracted aug-cc-pVQZ basis set, with additional functions for core correlation), as a function of the coupling parameter μ (a.u.): $(E_c^{DFT}(sr) + E_c^{CCSD(T)}(lr))/E_c^{CCSD(T)}$ is the ratio of the mixed *sr*-DFT/*lr*-CCSD(T) correlation approximation, with the LDA and our modified PBE-like functional, to the full CCSD(T) correlation energy.

3. Results and discussion

The calculation of van der Waals interactions poses a great challenge both to density functional and to ab initio methods. Current density functional approximations often provide quite unreliable results for these systems, especially for the dispersion interaction of non-overlapping entities, whereas ab initio methods like coupled-cluster theory are capable of yielding very accurate results but require large basis sets to reach the correct limit.

In order to systematically study the new spin density functional we applied it to alkali-metal rare-gas dimers; for this purpose we determined bond lengths R_e, dissociation energies D_e and harmonic wavenumbers ω_e for each alkali-metal rare-gas dimer AmRg (Am = Li–Cs; Rg = Ne–Xe) by calculating seven counterpoise corrected [13] energy points equally spaced with distances of 0.1 Å around the minimum of the potential curve and approximating them with a function of the form $\sum_{i=-1}^{4} a_i R^i$ by means of a least-squares-fit. In the case of the second and third row elements these results were obtained in all-electron calculations using correlation consistent polarised valence triple zeta (cc-pVTZ) basis sets for Li and Na

[14] and augmented cc-pVTZ (aug-cc-pVTZ) basis sets for Ne and Ar [15–18]. In the case of the heavier elements we employed small-core relativistic effective core potentials (RECPs) [19,20] in connection with the associated aug-cc-pVTZ basis sets for Kr and Xe, and the spdf part of the associated basis sets for K, Rb and Cs, respectively. We will refer to these basis sets as basis A. For the Rg atoms, we correlated the valence shell in the *lr*-CCSD(T) calculations; for the Am atoms, we also included outer-core correlation. If experimental results were available [21–29], we compared these with our theoretically predicted values. For the Li and Na compounds, where correlation consistent basis sets up to quintuple zeta quality are available [14–18,30], we also compared to basis set extrapolated CCSD(T) values. We calculated these values from the (aug-)cc-pV5Z Hartree–Fock energies and from extrapolations of the (aug-)cc-pVXZ ($X = 4,5$) correlation energies to the complete basis set limit (CBS[45]) according to $E_c = E_{CBS} + aX^{-3}$ [31]. The resulting theoretical reference values agree very well with experiment. The mean absolute deviations (MADs) between the experimental data and the basis set extrapolated values are 0.025 Å for R_e and 3.4 cm^{-1} for D_e.

In order to link the values of the coupling parameter μ to the densities of the systems under consideration, we used the relation $\mu = 2/R_e$ for the Rg dimers in our previous work [5]. For the alkali-metal rare-gas dimers, the situation is more complicated, since these systems comprise quite different densities and length scales. The atomic radii of the alkali atoms are much larger than those of the Rg atoms. Moreover, we have a substantial contribution to the binding energy from the alkali-metal cores, i.e., from entities which are much smaller again than the Am valence shells. In order to cope with this situation, we found it reasonable to work with a system-averaged μ value. Such a value has been determined by Ángyán and co-workers in *sr*-DFT/*lr*-HF calculations for the members of the G2 test set [32] and been applied in *sr*-DFT/*lr*-MP2 calculations for van der Waals molecules [33,34]. For the present work, we adopted his μ value of 0.5. We demonstrate below that the sensitivity of the results on the chosen μ value is not overly large.

Let us first compare our best results with the mixed method at $\mu = 0.5$ (*sr*-PBE/*lr*-CCSD(T)) with the pure PBE and pure CCSD(T) limits, calculated with basis A. The bond lengths R_e, dissociation energies D_e and harmonic wavenumbers ω_e are listed in Tables 1–3 (first, third and fifth column) and compared to the theoretical and experimental reference data (sixth and seventh column). It is seen that the *sr*-PBE/*lr*-CCSD(T) results are accurate to ≈0.07 Å for R_e, ≈5 cm^{-1} for D_e, and 1 cm^{-1} for ω_e, when compared to experiment; the maximum deviations are 0.18 Å for R_e (NaNe) and 24 cm^{-1} for D_e (NaXe – note that the experimental uncertainty is quite large for this molecule). When compared to the theoretical reference data, the situation is even more favourable, with MADs of ≈0.04 Å for R_e, ≈2 cm^{-1} for D_e, and <1 cm^{-1} for ω_e. The maximum deviations for R_e (≈0.1 Å) are dominated by the very weakly bound Ne compounds; for D_e, the largest errors arise for the Xe compounds, i.e., the molecules with the largest absolute D_e values (≈7 cm^{-1} for NaXe,

Table 1
Bond lengths R_e (Å) of the AmRg dimers from standard DFT calculations with PBE functional, mixed *sr*-PBE/*lr*-CCSD, *sr*-PBE/*lr*-CCSD(T), *sr*-LDA/*lr*-CCSD(T) calculations and standard CCSD(T) calculations with basis A, and from basis set extrapolated standard CCSD(T) calculations

	Basis A					CBS[45]	Experimental
	PBE	PBE/CCSD	PBE/CCSD(T)	LDA/CCSD(T)	CCSD(T)	CCSD(T)	
LiNe	4.389	5.314	5.310	5.344	5.608	5.226	
LiAr	4.845	4.890	4.870	4.899	5.104	4.896	4.893 (8) [22]
LiKr	4.679	4.791	4.764	4.789	4.988	4.807	4.78 (3) [23]
LiXe	4.680	4.868	4.831	4.861	5.030	4.844	4.80 (2) [23]
NaNe	4.399	5.475	5.470	5.499	5.839	5.366	5.29 (5) [24]
NaAr	4.900	5.020	4.998	5.024	5.291	5.005	5.01 (1) [25]
NaKr	4.753	4.914	4.885	4.907	5.153	4.914	4.918 (4) [26]
NaXe	4.832	5.004	4.965	4.992	5.200	4.965	4.95 (4) [27]
KNe	4.547	5.986	5.967	6.010	6.319		
KAr	5.096	5.377	5.322	5.366	5.615		5.404 (5) [28]
KKr	4.954	5.188	5.137	5.162	5.425		5.24 [29]
KXe	5.123	5.281	5.217	5.247	5.467		5.25 [29]
RbNe	4.636	6.212	6.192	6.224	6.553		
RbAr	5.189	5.498	5.447	5.482	5.784		
RbKr	5.042	5.269	5.207	5.235	5.541		5.29 [29]
RbXe	5.239	5.368	5.294	5.325	5.700		
CsNe	4.667	6.502	6.461	6.514	6.863		
CsAr	5.237	5.659	5.591	5.633	5.954		5.50 [29]
CsKr	5.103	5.367	5.282	5.315	5.666		5.44 [29]
CsXe	5.336	5.469	5.371	5.409	5.700		5.47 [29]
MAD	0.318/0.233	0.037/0.050	0.038/0.069	0.043/0.060	0.274/0.267		

Experimental data are taken from Refs. [22–29], errors in the last digits (if known) are quoted in parentheses. In each case, mean absolute deviations with respect to complete basis set extrapolated values and experimental data are given in the form .../....

Table 2
Dissociation energies D_e (cm^{-1}) of the AmRg dimers from standard DFT calculations with PBE functional, mixed *sr*-PBE/*lr*-CCSD, *sr*-PBE/*lr*-CCSD(T), *sr*-LDA/*lr*-CCSD(T) calculations and standard CCSD(T) calculations with basis A, and from basis set extrapolated standard CCSD(T) calculations

	Basis A					CBS[45]	Experimental
	PBE	PBE/CCSD	PBE/CCSD(T)	LDA/CCSD(T)	CCSD(T)	CCSD(T)	
LiNe	35.8	5.9	6.0	5.8	4.0	7.4	
LiAr	34.3	38.7	40.3	39.1	28.0	41.1	42.15 (20)
LiKr	50.1	64.1	67.6	65.8	48.8	67.2	68 (8)
LiXe	59.9	88.3	94.8	91.8	73.6	100.9	102 (2)
NaNe	38.9	5.8	5.8	5.7	3.8	7.1	8.1 (9)
NaAr	37.3	38.1	39.7	38.6	27.0	40.5	41.6 (2)
NaKr	55.3	63.3	66.9	65.1	47.5	66.9	68.4 (5)
NaXe	64.0	86.5	93.0	90.1	71.4	99.6	117 (15)
KNe	53.9	5.5	5.6	5.5	3.7		
KAr	48.9	39.2	41.7	40.4	28.2		40.1 (6)
KKr	74.3	67.9	73.5	71.5	51.1		71
KXe	80.7	92.5	102.0	98.7	76.7		111
RbNe	55.3	4.9	5.0	4.9	3.3		
RbAr	51.6	35.9	38.6	37.3	25.5		
RbKr	78.7	65.2	71.3	69.3	48.1		73
RbXe	83.7	89.3	99.5	96.3	76.7		
CsNe	65.1	4.5	4.7	4.5	3.1		
CsAr	60.1	36.2	39.6	38.2	26.0		45
CsKr	91.4	68.1	75.9	73.6	50.5		74
CsXe	94.5	93.2	106.0	102.2	76.7		110
MAD	21.9/18.9	5.0/8.9	2.2/4.7	3.6/5.9	15.8/22.4		

Experimental data are taken from Refs. [22–29], errors in the last digits (if known) are quoted in parentheses. In each case, mean absolute deviations with respect to complete basis set extrapolated values and experimental data are given in the form .../....

which is significantly smaller than the corresponding deviation from experiment). Note that the *sr*-PBE/*lr*-CCSD(T) results are not just an interpolation between the results of the limiting methods: whereas the R_e values of the mixed method are mostly intermediate between the PBE and CCSD(T) limits, the D_e values of the mixed method are

Table 3
Harmonic wavenumbers ω_e (cm^{-1}) of the AmRg dimers from standard DFT calculations with PBE functional, mixed *sr*-PBE/*lr*-CCSD, *sr*-PBE/*lr*-CCSD(T), *sr*-LDA/*lr*-CCSD(T) calculations and standard CCSD(T) calculations with basis A, and from basis set extrapolated standard CCSD(T) calculations

	Basis A					CBS[45]	Experimental
	PBE	PBE/CCSD	PBE/CCSD(T)	LDA/CCSD(T)	CCSD(T)	CCSD(T)	
LiNe	19.5	8.9	9.0	8.8	7.2	10.2	
LiAr	17.8	21.0	21.4	21.1	17.8	21.8	21.7
LiKr	21.1	25.2	25.8	25.5	22.0	25.8	
LiXe	22.3	28.1	28.9	28.4	25.6	29.9	
NaNe	17.5	6.0	6.0	5.9	4.7	6.8	
NaAr	11.6	12.8	13.1	12.9	10.6	13.4	13.3
NaKr	13.9	14.6	14.9	14.7	12.4	15.1	14.9
NaXe	14.3	15.8	16.3	16.1	14.1	17.2	19.7
KNe	22.5	4.2	4.5	4.1	3.8		
KAr	13.4	8.8	8.9	8.5	8.4		10.0
KKr	12.1	10.9	11.3	11.1	9.5		
KXe	11.8	11.6	12.1	11.9	10.6		
RbNe	13.5	4.2	4.1	4.2	3.1		
RbAr	10.0	7.7	8.0	7.9	6.6		
RbKr	9.6	8.2	8.5	8.4	7.1		
RbXe	8.8	8.5	8.9	8.8	7.4		
CsNe	13.9	3.0	3.6	2.9	2.8		
CsAr	9.9	6.9	7.2	7.1	5.9		
CsKr	8.9	7.0	7.3	7.2	6.2		
CsXe	7.9	7.1	7.5	7.3	6.6		
MAD	5.3/3.1	1.0/1.3	0.6/1.0	0.8/1.3	3.2/3.3		

Experimental data are taken from Refs. [22–29]. In each case, mean absolute deviations with respect to complete basis set extrapolated values and experimental data are given in the form .../....

very often larger than both the PBE and CCSD(T) ones. Thereby, the mixed method clearly outperforms both the pure PBE method and the pure CCSD(T) method. The former leads to MAD values with respect to the experimental (theoretical) reference data of ≈0.23 (0.32) Å for R_e and ≈19 (22) cm^{-1} for D_e; although these deviations are much smaller than one would have anticipated (much smaller anyway than the LDA ones, cf. below), one should be aware of the fact that the error of the D_e results is quite unsystematic – the Ne compounds are overbound by factors of 4–5, while the Xe compounds are underbound by up to 40%. The pure CCSD(T) calculation gives MADs with respect to the experimental (theoretical) reference data of ≈0.27 (0.27) Å for R_e and ≈22 (16) cm^{-1} for D_e. Due to the limited size of the basis sets, these deviations are not better than those obtained with pure PBE, but the CCSD(T) deviations are much more systematic than the PBE ones.

Improving the basis set quality changes the situation. We enlarged basis A to approximately quadruple zeta quality as follows. For Li and Na, we used the cc-pVQZ basis sets; for K, we added a *g* function with an exponent of 0.172200, and for Rb and Cs we used the full spdfg basis sets of Ref. [20]. The Rg atoms were calculated with the aug-cc-pVQZ basis sets of Refs. [15–19]. With the resulting basis B, the CCSD(T) results become superior to the PBE ones. While the MADs of the PBE results remain virtually unchanged, the MADs with respect to experiment (or with respect to CBS[45]-CCSD(T)) of the CCSD(T) results are reduced to ≈0.15 (0.14) Å for R_e and ≈14 (8) cm^{-1} for D_e. In comparison, the MADs of the mixed *sr*-PBE/*lr*-CCSD(T) results are given by ≈0.10 (0.07) Å for R_e and ≈6 (5) cm^{-1} for D_e. This means that compared to the triple zeta results R_e deteriorates by 0.03 Å, whereas the quality of D_e remains essentially unchanged (the change is 1 (3) cm^{-1}). Admittedly, the basis set dependence of D_e looks better than it actually is, because either the results obtained with smaller and larger basis set, respectively, can be found on different sides of the experimental value or the differences between two such results have not the same sign for all molecules. Nevertheless, the *sr*-PBE/*lr*-CCSD(T) method surpasses the pure borderline cases also for the extended basis set. The large basis set dependence of the pure CCSD(T) results does not come as a surprise, since it is well known that the dispersion energy is very slowly convergent with respect to the basis set size. In particular, high angular momentum polarisation functions are required. Consequently, the CCSD(T) values obtained with the smaller basis sets are still quite far from the basis set limit. The basis set dependence of the *sr*-PBE/*lr*-CCSD(T) method is smaller, since not only intraatomic but also part of the interatomic interaction is described by *sr* DFT. Note that the results with the mixed method refer to shorter bond lengths (and larger correlation energies) than those with pure CCSD(T), which partially counteracts the favourable influence of the small basis set dependency of DFT.

Of course, a judicious choice of the coupling parameter μ is important: μ should not be too small in order not to lose too much accuracy with respect to CCSD(T); on the other hand, μ should not be too large in order to keep the basis set dependency reasonably small. However, it turns out that our results are not very sensitive with respect to a variation of μ; *sr*-PBE/*lr*-CCSD(T) calculations with a coupling parameter of $\mu = 0.4$ (which is about half-way between $\mu = 0.5$ and the μ values used for the rare gas dimers in Ref. [5]) show MADs of ≈0.12 (0.07) Å for R_e and ≈7 (3) cm^{-1} for D_e.

In order to study how a reduction of the theoretical level will affect the results, we performed *sr*-PBE/*lr*-CCSD and *sr*-LDA/*lr*-CCSD(T) (see Tables 1–3 second and fourth column) as well as pure LDA and CCSD calculations (not shown in the table). As expected, triple excitations are very important for standard CCSD(T) calculations – their omission worsens the MAD values by ≈0.2 Å for R_e and ≈10 cm^{-1} for D_e. By contrast, the effect of triple excitations on the *sr*-DFT/*lr*-ab initio calculations is significantly smaller, namely < 0.02 Å for R_e and 3–4 cm^{-1} for D_e. This is due to the fact that triple excitations from spatially close orbitals are taken over by DFT. But also the substitution of the PBE functional with the LDA functional only slightly affects the results of the *sr*-DFT/*lr*-ab initio calculations – the R_e MAD changes by <0.01 Å and the D_e MAD by ≈1 cm^{-1} only – which is even more remarkable, since pure LDA – with MADs of ≈1.25 Å for R_e and ≈250 cm^{-1} for D_e – is much worse than pure PBE.

4. Conclusions

The PBE-like short-range density functional, which was introduced in a previous paper for use in long-range ab initio coupled-cluster calculations, has been extended from closed-shell to open-shell cases. In line with previous results for the rare gas dimers, a systematic study for alkali-metal rare-gas dimers shows that with medium-size basis sets of triple (and even quadruple) zeta quality the mixed short-range PBE/long-range CCSD(T) method yields results superior not only to those of the standard PBE method but also to those of the standard CCSD(T) method.

Acknowledgements

The authors are grateful to the Deutsche Forschungsgemeinschaft (DFG) for a grant to E.G. within the Priority Program 1145 *Modern and universal first-principles methods for many-electron systems in chemistry and physics*. Financial support by the Alexander von Humboldt Foundation to T.L. and by the Fonds der Chemischen Industrie to H.-J.W. and H.S. is also gratefully acknowledged.

References

[1] H. Stoll, A. Savin, Density functionals for correlation energies of atoms and molecules, in: R. Dreizler, J. da Providencia (Eds.), Density Functional Methods in Physics, Plenum Press, New York, 1985, pp. 177–207.

[2] A. Savin, H.-J. Flad, Density functionals for the Yukawa electron–electron interaction, Int. J. Quantum Chem. 56 (1995) 327–332.
[3] T. Leininger, H. Stoll, H.-J. Werner, A. Savin, Combining long-range configuration interaction with short-range density functionals, Chem. Phys. Lett. 275 (1997) 151–160.
[4] J. Toulouse, F. Colonna, A. Savin, Long-range–short-range separation of the electron–electron interaction in density-functional theory, Phys. Rev. A 70 (2004) 062505.
[5] E. Goll, H.-J. Werner, H. Stoll, A short-range gradient-corrected density functional in long-range coupled-cluster calculations for rare gas dimers, Phys. Chem. Chem. Phys. 7 (2005) 3917–3923.
[6] J.P. Perdew, K. Burke, M. Ernzerhof, Generalized gradient approximation made simple, Phys. Rev. Lett. 77 (1996) 3865–3868.
[7] P. Knowles, C. Hampel, H.-J. Werner, Coupled cluster theory for high spin, open shell reference wave functions, J. Chem. Phys. 99 (1993) 5219–5227.
[8] P. Knowles, C. Hampel, H.-J. Werner, Erratum: coupled cluster theory for high spin, open shell reference wave functions [J. Chem. Phys. 99 (1993) 5219], J. Chem. Phys. 112 (2000) 3106–3107.
[9] H.-J. Werner, P. Knowles, MOLPRO is a package of ab initio programs designed by H.-J. Werner and P.J. Knowles, version 2002.10; R.D. Amos, A. Bernhardsson, A. Berning, P. Celani, D.L. Cooper, M.J.O. Deegan, A.J. Dobbyn, F. Eckert, C. Hampel, G. Hetzer, P.J. Knowles, T. Korona, R. Lindh, A.W. Lloyd, S.J. McNicholas, F.R. Manby, W. Meyer, M.E. Mura, A. Nicklass, P. Palmieri, R. Pitzer, G. Rauhut, M. Schütz, U. Schumann, H. Stoll, A.J. Stone, R. Tarroni, T. Thorsteinsson, and H.-J. Werner, 2006.
[10] M. Levy, Universal variational functionals of electron-densities, 1st-order density-matrices and natural spin–orbitals and solution of the V-representability problem, Proc. Natl. Acad. Sci. USA 76 (1979) 6062–6065.
[11] J. Toulouse, F. Colonna, A. Savin, Short-range exchange and correlation energy density functionals: beyond the local-density approximation, J. Chem. Phys. 122 (2005) 014110.
[12] S. Paziani, S. Moroni, P. Gori-Giorgi, G.B. Bachelet, Local-spin-density functional for multideterminant density functional theory, Phys. Rev. B 73 (2006) 155111.
[13] S.F. Boys, F. Bernardi, The calculation of small molecular interactions by the differences of separate total energies. Some procedures with reduced errors, Mol. Phys. 19 (1970) 553–566.
[14] D.E. Woon, K.A. Peterson, T.H. Dunning, Jr., Gaussian basis sets for use in correlated molecular calculations. VII. Valence and core–valence basis sets for Li, Na, Be, and Mg, in preparation.
[15] T.H. Dunning Jr., Gaussian basis sets for use in correlated molecular calculations. I. The atoms boron through neon and hydrogen, J. Chem. Phys. 90 (1989) 1007–1023.
[16] R. Kendall, T.H. Dunning Jr., R. Harrison, Electron affinities of the first-row atoms revisited. Systematic basis sets and wave functions, J. Chem. Phys. 96 (1992) 6796–6806.
[17] D. Woon, T.H. Dunning Jr., Gaussian basis sets for use in correlated molecular calculations. III. The atoms aluminum through argon, J. Chem. Phys. 98 (1993) 1358–1371.
[18] D. Woon, T.H. Dunning Jr., Gaussian basis sets for use in correlated molecular calculations. IV. Calculation of static electrical response properties, J. Chem. Phys. 100 (1994) 2975–2988.
[19] K.A. Peterson, D. Figgen, E. Goll, H. Stoll, M. Dolg, Systematically convergent basis sets with relativistic pseudopotentials. II. Small-core pseudopotentials and correlation consistent basis sets for the post-d group 16–18 elements, J. Chem. Phys. 119 (2003) 11113–11123.
[20] I.S. Lim, P. Schwerdtfeger, B. Metz, H. Stoll, All-electron and relativistic pseudopotential studies for the group 1 element polarizabilities from K to element 119, J. Chem. Phys. 122 (2005) 104103.
[21] P.F. Bernath, S. McLeod, DiRef, A database of references associated with the spectra of diatomic molecules, J. Mol. Spectr. 207 (2001) 287.
[22] R. Brühl, D. Zimmermann, High-resolution laser spectroscopy of LiAr: improved interaction potential and spin–rotation-coupling in the ground state X $^2\Sigma^+$, J. Chem. Phys. 115 (2001) 7892–7896.
[23] D.J. Auerbach, High resolution differential cross sections and intermolecular potentials I: Li–Kr and Li–Xe, J. Chem. Phys. 60 (1974) 4116–4122.
[24] W.P. Lapatovich, R. Ahmad-Bitar, P.E. Moskowitz, I. Renhorn, R.A. Gottscho, D.E. Pritchard, Laser spectroscopy of the diatomic von der Waals molecule NaNe, J. Chem. Phys. 73 (1980) 5419–5424.
[25] D. Schwarzhans, D. Zimmermann, High resolution laser spectroscopy of NaAr: improved interaction potential for the X $^2\Sigma^+$ ground state, Eur. Phys. J. D 22 (2003) 193–198.
[26] R. Brühl, J. Kapetanakis, D. Zimmermann, Determination of the Na–Kr interaction potential in the XΣ and AΠ state by laser spectroscopy, J. Chem. Phys. 94 (1991) 5865–5874.
[27] P. Baumann, D. Zimmermann, R. Brühl, Laser spectroscopic investigation of the van der Waals molecule NaXe, J. Mol. Spectr. 155 (1992) 277–297.
[28] F. Bokelmann, D. Zimmermann, Determination of the K–Kr interaction potential in the XΣ and AΠ state from laser spectroscopic data, J. Chem. Phys. 104 (1996) 923–934.
[29] U. Buck, H. Pauly, Interferenzen bei atomaren Stoßprozessen und ihre Interpretation durch ein modifiziertes Lennard-Jones-Potential, Zeit. f. Phys. 208 (1968) 390–417.
[30] Basis sets were obtained from the Extensible Computational Chemistry Environment Basis Set Database, Version 02/25/04, as developed and distributed by the Molecular Science Computing Facility, Environmental and Molecular Sciences Laboratory which is part of the Pacific Northwest Laboratory, P.O. Box 999, Richland, Washington 99352, USA, and funded by the US Department of Energy. The Pacific Northwest Laboratory is a multi-program laboratory operated by Battelle Memorial Institute for the US Department of Energy under contract DE-AC06-76RLO 1830. Contact Karen Schuchardt for further information.
[31] T. Helgaker, W. Klopper, H. Koch, J. Noga, Basis-set convergence of correlated calculations on water, J. Chem. Phys. 106 (1997) 9639–9646.
[32] I.C. Gerber, J.G. Ángyán, Hybrid functional with separated range, Chem. Phys. Lett. 415 (2005) 100–105.
[33] J.G. Ángyán, I. Gerber, A. Savin, J. Toulouse, van der Waals forces in density functional theory: perturbational long-range electron-interaction corrections, Phys. Rev. A 72 (2005) 012510.
[34] I.C. Gerber, J.G. Ángyán, Potential curves for alkaline-earth dimers by density functional theory with long-range correlation corrections, Chem. Phys. Lett. 416 (2005) 370–375.